Hindawi
Journal of Advanced Transportation
Volume 2018, Article ID 7905820, 19 pages
https://doi.org/10.1155/2018/7905820

Research Article

Integrated Optimization on Train Control and Timetable to Minimize Net Energy Consumption of Metro Lines

Yuhe Zhou[1], **Yun Bai**[1], **Jiajie Li**[1], **Baohua Mao**[1] and **Tang Li**[2]

[1]*MOE Key Laboratory for Urban Transportation Complex Systems Theory and Technology, Beijing Jiaotong University, Beijing 100044, China*
[2]*Department of Civil and Environmental Engineering, Imperial College London, London SW7 2AZ, UK*

Correspondence should be addressed to Yun Bai; yunbai@bjtu.edu.cn

Received 15 December 2017; Revised 21 February 2018; Accepted 19 March 2018; Published 26 April 2018

Academic Editor: Andrea D'Ariano

Energy-efficient metro operation has received increasing attention because of the energy cost and environmental concerns. This paper developed an integrated optimization model on train control and timetable to minimize the net energy consumption. The extents of train motoring and braking as well as timetable configurations such as train headway and interstation runtime are optimized to minimize the net energy consumption with consideration of utilizing regenerative energy. An improved model on train control is proposed to reduce traction energy by allowing coasting on downhill slopes as much as possible. Variations of train mass due to the change of onboard passengers are taken into account. The brute force algorithm is applied to attain energy-efficient speed profiles and an NS-GSA algorithm is designed to attain the optimal extents of motoring/braking and timetable configurations. Case studies on Beijing Metro Line 5 illustrate that the improved train control approach can save traction energy consumption by 20% in the sections with steep downhill slopes, in comparison with the commonly adopted train control sequence in timetable optimization. Moreover, the integrated model is able to significantly prolong the overlapping time between motoring and braking trains, and the net energy consumption is accordingly reduced by 4.97%.

1. Introduction

Metro systems develop rapidly across the world because of their high reliability and large capacity. For example, the total length of metro lines in mainland China was only about 1500 km in 2010 and more than 3700 km in 2016 and is expected to reach 6000 km by 2020. Although the metro is one of the most energy-efficient transport means, the long operating mileage and high traffic volume make the total energy consumption of metro systems become significant. Metro operators are facing more pressure to save energy due to increasing environmental concerns and operational costs. Energy-efficient train control and service timetable optimization are preferred to reduce metro train energy consumption in existing urban rail systems, as significant energy saving could be achieved with relatively low capital investment and minor modifications [1].

Energy-efficient train control (EETC) has been widely applied to real-world train operation since the 1980s. It aims to find the optimal sequence of train control modes and the switching points among the modes. Ichikawa [2] pointed out that energy-efficient train control on level tracks includes maximum acceleration (MA), cruising (CR), coasting (CO), and maximum braking (MB). Strobel et al. [3] found that it is also applicable to trains running in downhill and uphill sections with small slopes, where partial motoring and braking might be implemented to maintain cruising. Milroy [4] concluded that cruising is not necessarily required in short interstation runs. Subsequently, Benjamin et al. [5] and Howlett et al. [6] demonstrated that coasting presents opportunities for energy saving especially in long interstation runs. Khmelnitsky [7] researched the optimal operation of a train on a variable grade profile subject to arbitrary speed restrictions and presented a numerical algorithm to find the optimal velocity profile. Liu and Golovitcher [8] gave the analytical solution of optimal control and equations to find the control change points; speed limit and steep gradients are taken into account. Dongen and Schuit [9] and Scheepmaker

and Goverde [10] proposed two models to find the optimal cruising speed and the proper coasting location to minimize energy consumption for train interstation runs.

In recent years, Howlett et al. [11] proposed energy-efficient control approaches for freight trains on steep tracks. Their survey indicated that coasting before a steep downhill section is very important for energy saving. Bai et al. [12] found that up to 9% of the energy consumption for train interstation runs could be saved by applying coasting as much as possible before braking. Domínguez et al. [13] and Carvajal-Carreño et al. [14] presented approaches to attain the optimal schemes of the ATO speed profile to obtain the Pareto front between train runtime and energy consumption. Sicre et al. [15] considered a specific model for energy-efficient manual driving in high speed lines by means of fuzzy parameters; uncertainty in manual control and punctuality requirement are taken into account. Keskin and Karamancioglu [16] attached more importance to train mass and compared the effectiveness of different evolutionary algorithms in attaining solutions for energy-efficient train control. Shangguan et al. [17] developed a multiobjective optimization approach for single-train speed trajectory.

Energy-efficient train timetabling (EETT) aims to reduce the net energy consumption of metro lines via optimizing the timetable configurations, such as the distribution of runtime supplements among different interstations, dwell time at stations, and train headways. Albrecht and Oettich [18] applied dynamic programming to find the optimal timetable considering both train energy consumption and passenger waiting time. Sicre et al. [19] attained the Pareto curves of journey time and energy consumption for high speed train interstation itinerary and then optimized the distribution of runtime supplements among different interstations. Chevrier et al. [20] proposed a biobjective evolutionary algorithm to attain speed profiles for train interstation runs in which runtime and energy consumption were optimized concurrently.

EETT has become more popular in recent years with the application of regenerative braking [21], which is able to convert kinetic energy into electricity during train braking. Regenerative electricity could provide up to 40% of the energy supplied to trains [22]. The regenerative energy is firstly used to support onboard auxiliary devices of the braking train and then fed back into the overhead contact line to assist motoring and auxiliary equipment of other trains in the same power supply interval (PSI). If the feedback energy cannot be used in time, it will be consumed by protective resistor, as most metro systems have not installed energy storage devices. The motoring and braking trains could be synchronized for better utilization of regenerative energy by optimizing timetable configurations, which determine train motoring and braking timing when the train departs from and approaches stations. Albrecht [23] explored the optimal allocation of runtime supplement for train interstation runs, to minimize the net energy consumption and reduce the maximal load of power systems. Yang et al. [24] built a model to maximize the overlapping time between the motoring and braking of successive trains by regulating train headway and dwell time. Further, Yang et al. [25] and Le et al. [26] proposed models to maximize the utilization of regenerative braking energy (RBE) as well. Peña-Alcaraz et al. [27] designed a mathematical programming model to synchronize the braking of trains arriving at station with the acceleration of trains exiting from the same or another station.

More energy saving could be achieved by integrated optimization on train timetable and control scheme. Ding et al. [28] proposed a two-level optimization model to find the energy-efficient train trajectory as well as the distribution of runtime supplements to minimize the traction energy without changing the predefined journey time. Su et al. [29, 30] developed an integrated optimization model, consisting of both train control and timetable formulation, to minimize the total energy consumption of multiple trains. Yang et al. [31] developed a stochastic programming model for the integrated optimization on train timetable and speed profile, where train mass in each interstation was set as a stochastic variable with a given probability distribution. Li and Lo [32] developed an integrated model on train control and timetable formulation to minimize the net energy consumption, where regenerative braking was taken into account. Zhao et al. [33] presented an integrated optimization model on train trajectory and timetable to reduce the net energy consumption and peak power of substations; the effectiveness of the proposed model was verified by a multiple-train movement simulator.

Many previous researches have explored the integrated optimization of train operation for energy saving, including both train control and timetabling, especially for the metro lines where RBE is available. In these studies, the maximum traction and braking force are commonly applied in train control. However, partial traction and braking when trains depart from and approach stations are able to improve the utilization of regenerative energy via prolonging train motoring and braking time, at the expense of a slight increment of traction energy consumption. Moreover, the EETC applied in EETT is usually based on the control sequence of MA-CR-CO-MB. Howlett et al. [11] proved that CR-CO-CR saves more energy than the control scheme of only CR when the train runs on steep downhill slopes. Liu and Golovitcher [8] also presented an equation to derive the conditions where different control modes should be applied with consideration of steep downhill slopes. Nevertheless, these improved train control strategies have not been employed in energy-efficient timetable optimization problems.

In this paper, an integrated optimization model on train control and timetable is developed to minimize the system net energy consumption, considering both traction energy reduction and utilization of regenerative braking energy. Synchronization of motoring and braking trains to better use the regenerative braking energy is realized by optimizing the extents of train motoring and braking as well as timetable configurations including headway and scheduled interstation runtime. An improved train control model allowing coasting on downhill slopes as much as possible is proposed to further reduce traction energy consumption compared with the simple control sequence of MA-CR-CO-MB, which is commonly adopted in previous energy-efficient timetabling studies. The proposed model takes into account the practical operation conditions such as varied train mass in different interstations, power peak of traction power supply system,

Table 1: Literature on energy-efficient timetabling with RBE.

Publication	Objective(s)	Variables	Speed profile	Mechanical braking	Power peak	Auxiliary devices	Varied mass
Albrecht (2004)	Power peak + energy consumption	Trip time	MA-CO-MB		√		
Peña-Alcaraz et al. (2011)	Overlapping time	Arrival & departure time			√	√	
Li and Lo Hong (2014)	Net energy consumption	Speed profile, headway, arrival & departure time	MA-CO-MB				
Yang et al. (2015)	Net energy consumption	Dwell time	MA-CO-MB			√	
Yang et al. (2016)	Traction energy	Speed profile, arrival & departure time	MA-CO-MB				√
Su et al. (2016)	Traction energy	Varied train characteristic	MA-CO-MB	√	√	√	√
Zhao et al. (2017)	Substation energy consumption	Speed profile, interstation journey time, service intervals	MA-CO-MB		√		
This paper	Net energy consumption	Speed profile, headway, interstation runtime	MA-$[CO\text{-}CR]_n$-MB	√	√	√	√

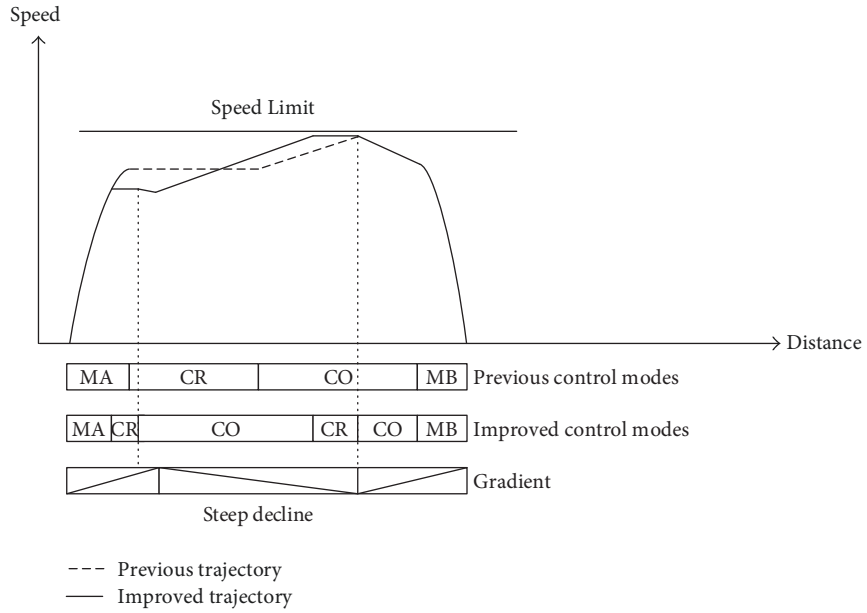

Figure 1: The improvements of the energy-efficient train control strategy.

and application of mechanical braking when the train adopts brakes at a very high speed. Table 1 gives a comparison between this study and the existing literatures.

The rest of this paper is organized as follows. In Section 2, an improved model on energy-efficient train control is presented. In Section 3, the integrated optimization model taking into account energy-efficient train control is developed to minimize the net energy consumption of a whole metro line. In Section 4, the brute force algorithm and an NS-GSA algorithm are presented to attain the optimal train trajectory and timetable, respectively. In Section 5, case studies on Beijing Metro Line 5 are conducted to verify the effectiveness of the proposed approach. Conclusions are provided in Section 6.

2. Energy-Efficient Train Control

There is usually more than one control scheme to drive a train from one station to the next even with the same runtime. The energy-efficient train control is to find the optimal control scheme leading to the minimal traction energy consumption while the scheduled runtime and speed limits are respected. Most previous studies proposed that the energy-efficient train control consists of the following four successive modes (i.e., MA, CR, CO, and MB) in the interstation with constant speed limit and no steep slopes, as illustrated by the dashed line in Figure 1.

With such a control, the train adopts maximum motoring followed by cruising at a constant speed and then coasting

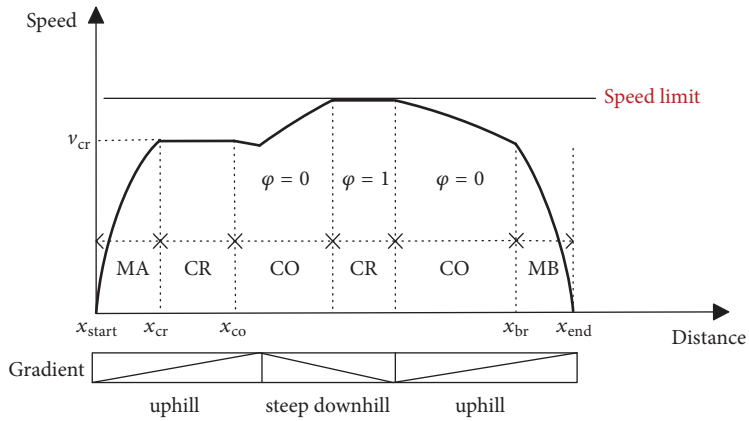

Figure 2: Improved energy-efficient train control scheme.

till braking for station stops. However, trains must brake to keep the speed constant in steep downhills, which is not preferred to minimize traction energy. The train could start cruising earlier and then adopt coasting on downhill slopes, followed by employing cruising and coasting again before stop braking, as illustrated by the solid line in Figure 1. As such, the energy consumption of the train interstation run could be saved, as the time for MA in the new trajectory is shortened while the interstation runtime remains the same. To this end, an improved model on train control is proposed to reduce the traction energy consumption by taking the full advantage of potential energy in downhill tracks, with the assumption that there is no change of speed limit in the whole interstation run.

2.1. Objective Function. The train adopts MA and MB in accelerating from and approaching stations in the proposed train control model, while the pairs of CR and CO are implemented in the interstation runs, as shown in Figure 2. It should be noted that Figure 2 is a sketch and switching points among different control modes might not be precise. With the proposed model, train control scheme is based on MA-$[\text{CR-CO}]_n$-MB and the positive integer n represents the number of CR and CO in one interstation journey. n is equal to 1 in most cases and the control scheme is MA-CR-CO-MB, which is the same as that attained by the previous model. n might be greater than 1 when the train is running on steep downhill tracks. Therefore, the proposed model is a supplement to previous work and it could contribute toward energy saving in the interstations with steep downhill profiles since more coasting is allowed.

The decision variables in the improved model are two switching points during one interstation run. The first point is the location where the first CR is applied, that is, x_{cr}. The second point is the location where the first CO is applied, that is, x_{co}. The other switching locations could be obtained once the decision variables are known. For example, the location to start the second CR is where the train reaches the speed limit. The train continues CR till it leaves the steep downhill slopes and CO is implemented again when the train does not accelerate with no traction power. The location to start applying MB, which is denoted by x_{br}, depends on the intersection point of coasting and braking profiles before the station stop. The objective function of the proposed model is to minimize the traction energy consumption for one interstation run, which is described as

$$\min \quad E_{\text{trac}}(x_{cr}, x_{co}) = \frac{\sum_{x=0}^{X} \max(\mathbf{F}(v,x), 0)}{3600 \cdot \eta_1}, \tag{1}$$

where E_{trac} is traction energy consumption with the given x_{cr} and x_{co} which are decision variables in EETT; η_1 is the energy conversion efficiency factor from electrical to mechanical energy; X is the length of one interstation; the units for distance, force, power, energy, and time are defined as m, kN, kW, kWh, and s in this paper; $\mathbf{F}(v,x)$ stands for the output force acting upon the train given by ATO. A positive value of $\mathbf{F}(v,x)$ denotes that the train is motoring. Zero indicates that the train is coasting and a negative value represents braking.

Traction force and braking force are expressed as a vector force that can be described as

$$\mathbf{F}(v,x) = \begin{cases} F_{\text{tr}}(v,x) & 0 \le x \le x_{cr} \\ F_{\text{cr}}(v,x) & x_{cr} < x \le x_{co} \\ \varphi \cdot F_{\text{cr}}(v,x) & x_{co} < x \le x_{br} \\ -F_{\text{br}}(v,x) & x_{br} < x \le X, \end{cases} \tag{2}$$

where $\mathbf{F}(v,x)$ is a vector force which is greater than 0 in traction mode or less than 0 in braking mode; $F_{\text{tr}}(v,x)$ is the maximum available traction force according to motor characteristic; $F_{\text{cr}}(v,x)$ is the force to keep cruising at position x; $F_{\text{br}}(v,x)$ is the maximum available braking force; φ is a binary variable with no unit.

$\varphi = 0$ indicates that the train control mode is CO, while $\varphi = 1$ stands for the case in which the control mode is CR. For example, coasting is implemented when the train arrives at x_{co} and φ is thus set as 0. When train speed increased to the limit, CR will be implemented again and φ becomes 1. Then resistance force F_R is used to decide the following

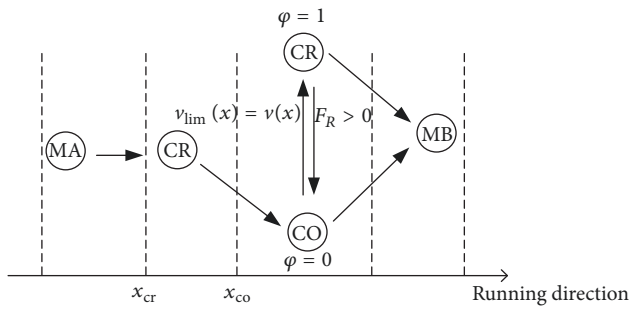

Figure 3: Transitions of train control modes with the improved model.

control regimes. φ can be therefore attained by the following equation:

$$\varphi(x) = \begin{cases} 0 & (v_{\lim}(x) - v(x)) + \varphi(x - \Delta x) \cdot F_R(v, x) > 0 \\ 1 & (v_{\lim}(x) - v(x)) + \varphi(x - \Delta x) \cdot F_R(v, x) \le 0, \end{cases} \quad (3)$$

where $v_{\lim}(x)$ and $v(x)$ are speed limit and train speed at position x, respectively. $\varphi(x-\Delta x)$ represents the train control mode in the previous distance step, where Δx represents the length of distance step. $F_R(v, x)$ is resultant resistance, consisting of friction resistance, air drag, and additional resistance caused by grades and curves.

Figure 3 demonstrates the possible transitions among different control modes. At the beginning stage, MA should be applied till the location where the train starts cruising, which is the first decision variable x_{cr}. In the mode of CR, the effort acting upon the train by ATO is equal to the resistance to keep train speed constant. Train continues its travel at a constant speed till it reaches the location to start CO, which is the second decision variable x_{co}. The following driving mode depends on train speed and running resistance according to (3). If train speed $v(x)$ does not exceed the speed limit $v_{\lim}(x)$, coasting phase will be continued. If train speed exceeds the limit, cruising phase will be adopted again. The coasting will be applied again only when the resultant resistance is positive, which indicates train speed decreases when coasting is applied. Finally, MB is applied before the station stop and the braking curve is attained by backward calculation from the target stop point using the maximum available braking effort.

According to the characteristics of train motor, the traction force varies with train speed. When MA is applied, there are three traction force curves to be chosen automatically in response to three train weights, as shown in Figure 4(a). When the train is empty, the traction force curve of AW0, which is the lowest one among all the three curves, is chosen because the train does not need too much traction force for acceleration. In case the number of passengers on the train is equal to the nominal capacity, the traction force curve of AW1 is adopted to allow a bigger acceleration rate than that of AW0. The traction force curve of AW2, which is the highest one, is selected when the train carries the most passengers. For the circumstances in which the actual train weight is not equal to one of the three weights above, the traction force is calculated as follows.

Firstly, we need to calculate train mass to obtain the available traction force.

$$m(x) = M_{\text{train}} + \mu \cdot \tau(n), \quad (4)$$

where $m(x)$ is the actual train mass; M_{train} is the rolling stock mass; $\tau(n)$ is the number of passengers on the train in the interstation of n; μ is the average mass of a person.

Secondly, linear interpolation is used to attain the practical traction force, as shown in

$$F_{\text{tr}}(v, x) = \begin{cases} F_0(v) + (F_1(v) - F_0(v)) \cdot \dfrac{m(x) - M_0}{M_1 - M_0} & M_0 \le m(x) < M \\ F_1(v) + (F_2(v) - F_1(v)) \cdot \dfrac{m(x) - M_1}{M_2 - M_1} & M_1 \le m(x) \le M_2, \end{cases} \quad (5)$$

where M_0, M_1, and M_2 represent train masses when the train is empty, nominally loaded, and maximum loaded, respectively; $F_0(v)$, $F_1(v)$, and $F_2(v)$ indicate the traction force in the above three circumstances.

Train mass also has impacts on train braking force. There are usually three different braking force curves corresponding to three different load factors, that is, AW0-AW1-AW2. The braking force under different load factors can be calculated similarly. However, the braking force usually keeps constant when train speed varies [34–36]. It should be noted that the practical braking force (F_{br}) is the combination of both mechanical braking and regenerative braking. Figure 4(b) shows the components of braking force, taking the case of AW1 as an example. Regenerative braking force (F_{eb}) declines gradually when train speed becomes very large or very small, and mechanical braking (F_{mech}) is applied to compensate the shortage of braking force.

As the traction force $F_{\text{tr}}(v, x)$ and braking force $F_{\text{br}}(v, x)$ are obtained, the traction energy consumption can be calculated by (1) and (2) once we obtained the value of $F_{\text{cr}}(v, x)$. The resultant force $F(v, x)$ acting upon the train can be calculated as

$$\begin{aligned} F(v, x) &= \mathbf{F}(v, x) - F_R(v, x) \\ F_R(v, x) &= R_{\text{basic}}(v) + R_{\text{grad}}(x) + R_c(x), \end{aligned} \quad (6)$$

where $R_{\text{basic}}(v) = a + bv + cv^2$ and the coefficients of a, b, and c are usually given by rolling stock manufacturers; $R_{\text{grad}}(x)$ is the resistance caused by the gradient; $R_c(x)$ is the resistance caused by the curve.

When cruising is applied, the resultant force $F(v, x)$ should be equal to zero; then, $F_{\text{cr}}(v, x)$ can be obtained based on Newton's law of motion:

$$\begin{aligned} F_{\text{cr}}(v, x) &= F_R(v, x) \\ &= m(x)\, g \cdot \left[\left(a + bv + cv^2 \right) + \sin\theta_x + \frac{600}{r_x} \right], \end{aligned} \quad (7)$$

where g is gravitational acceleration; θ_x is the angle of slope (negative means downhill); r_x is the radius of the curve at location x.

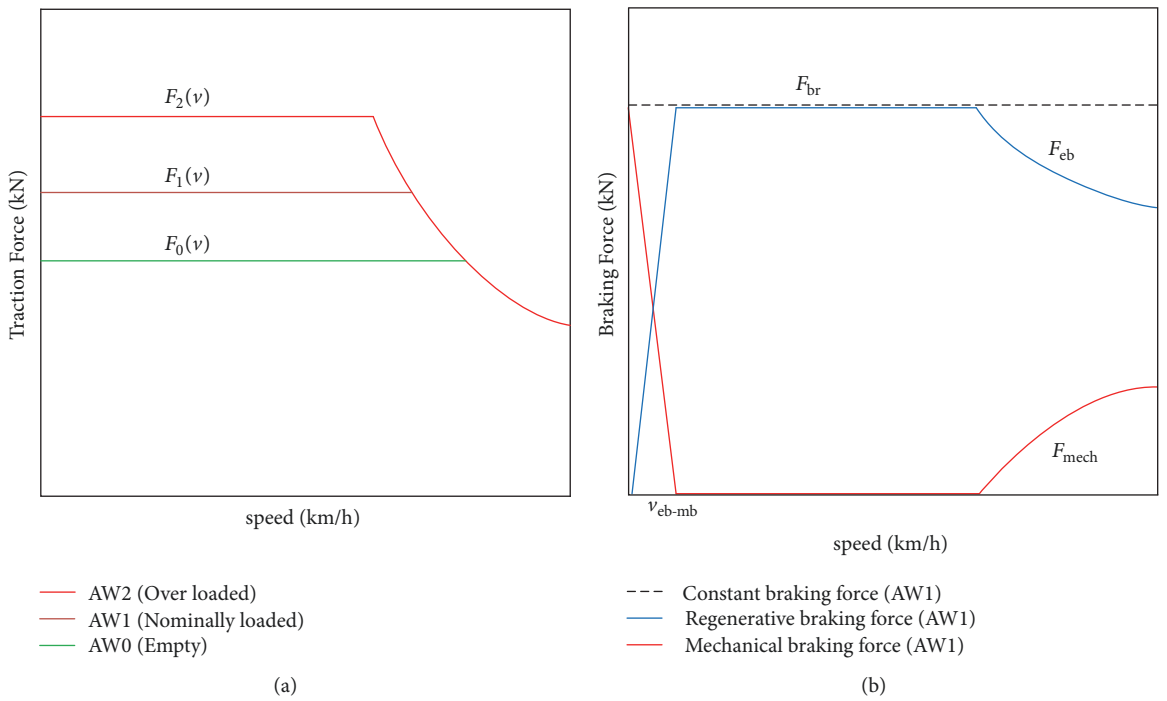

FIGURE 4: Maximum force against train speed. (a) Maximum traction force with different load factors. (b) Available braking forces in AW1.

2.2. Constraints. Train control schemes should be subject to the following constraints.

(1) For operational safety and passenger comfort, the acceleration should be limited within a proper range:

$$a_{\text{dec}} \leq \frac{dv(x)}{dt} \leq a_{\text{acc}}. \tag{8}$$

(2) The train must stop when it arrives at a station:

$$v(x_n) = 0, \quad \forall n \in [1, 2N]. \tag{9}$$

(3) Train velocity must not exceed the speed limit or be negative:

$$0 \leq v(x) \leq v_{\text{lim}}(x). \tag{10}$$

(4) The error between practical runtime and scheduled runtime should be less than a certain threshold. In this paper, we set this threshold as $\delta = 0.5$:

$$\left| \text{RT}_n - \sum_{x=x_n}^{x_{n+1}} \frac{\Delta x}{v(x)} \right| \leq \delta, \tag{11}$$

where RT_n is the scheduled runtime in interstation n; x_n refers to the location of station n.

(5) This constraint aims to calculate regenerated braking energy for timetable optimization in Section 3. As a matter of fact, regenerative braking force varies with train speed as well as load factor, and it will be entirely replaced by mechanical braking when train speed is lower than $v_{\text{eb-mb}}$.

$$F_{\text{eb}}(v, x) = \begin{cases} \min\left(F_{\text{eb}}(v, x), F_{\text{br}}\right), & v \geq v_{\text{eb-mb}} \\ 0, & v < v_{\text{eb-mb}}. \end{cases} \tag{12}$$

3. Integrated Optimization Model on Train Control and Timetable

With the application of regenerative braking, synchronization of motoring and braking trains in the same PSI for better utilization of regenerative energy becomes very important in minimizing the net energy consumption of metro lines, since the regenerative energy can provide a significant proportion of the total energy fed into rolling stocks. Train control also has a great influence on timetable optimization, as different control schemes lead to different energy consumption even when the interstation runtime remains the same.

An integrated model on train control and timetable optimization is proposed in this section to minimize the net energy consumption, taking into account the improved train control model described in Section 2. Train headway and interstation runtimes are optimized to improve the utilization of RBE as well as reduce the traction energy consumption by allocating the runtime supplements properly. In addition, power control system could be modified to constrain the output of traction and braking force when trains depart from and approach stations, which is able to enlarge the space for synchronization of motoring and braking trains via prolonging train motoring and braking time, although traction energy consumption increases slightly. Different from the previous studies, the new integrated model allows the train to adopt partial motoring and braking in accelerating from and approaching stations.

Figure 5 illustrates the influences on energy consumption by train headway, interstation runtime, and percentages of the full traction and braking force applied in train control. The motoring of train B and the braking of train A could be

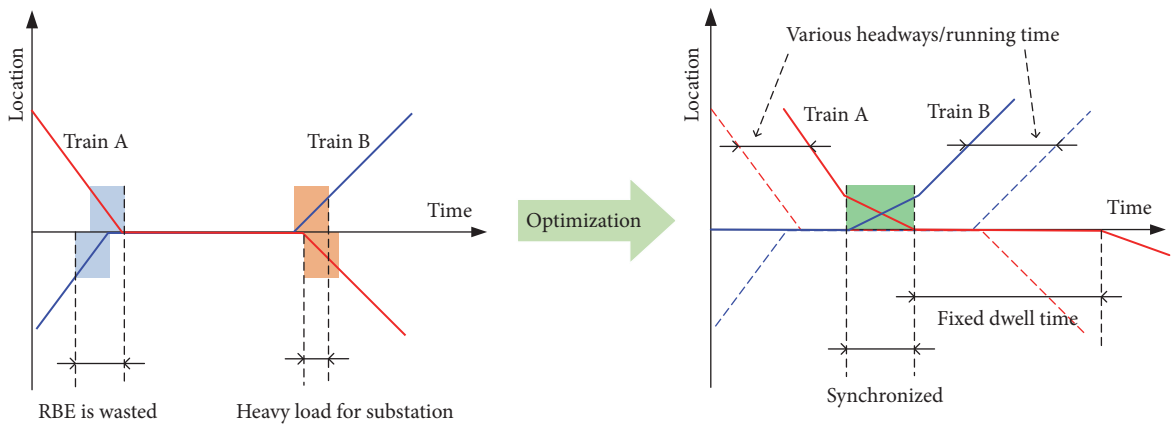

Figure 5: Energy-saving methods in integrated optimization.

synchronized by regulating train headway and interstation runtime; therefore, the regenerated energy produced by braking train A can be transferred to and utilized by traction train B. As a result, net energy consumption is reduced because the energy used in the accelerating phase of train B is provided by the regenerative braking of train A. The overlapping time, which means the time slot in which a train adopts regenerative braking while there is at least one train motoring in the same PSI, is further extended using partial traction and braking force.

Net energy consumption could be saved due to the much higher utilization of RBE, although the traction energy consumption may increase slightly. It should be pointed out that dwell time is not allowed to be changed in the integrated optimization model because it usually depends on the number of passengers getting on and off the train.

3.1. Objective Function. In this study, the whole problem of energy-efficient train operation is decomposed into train trajectory formulation and timetable optimization, which are successively processed. Firstly, train control scheme in each interstation run is optimized with the given runtime (RT), k_t, and k_b. Secondly, a database, including the optimal train control scheme and the corresponding energy consumption with all possible groups of RT, k_t, and k_b, is then built. Finally, the optimal HD, RT, k_t, and k_b are obtained by an evolutionary algorithm on the basis of the database. It should be noted that k_t and k_b are assumed as two constants for the sake of calculating efficiency and convenience of train control implementation.

The objective of the integrated model is to find the optimal utilization coefficients of traction and braking force (k_t, k_b), interstation runtime (RT), and headway (HD) to minimize the net energy consumption for all trains $j \in \{1, 2, 3, \ldots, J\}$ operating on the whole line, which is the difference between the required traction energy and the utilized regenerative energy. Additionally, energy consumed for auxiliary devices is also taken into account. The objective function is expressed as

$$\begin{aligned} \min \quad & E\left(k_t, k_b, \mathrm{RT}, \mathrm{HD}\right) \\ & = \sum_{j=1}^{J} \sum_{n=1}^{2N} E_{\mathrm{trac}}^{n,j}\left(k_t, k_b, \mathrm{RT}_n\right) + E_{\mathrm{aux}} \\ & \quad - \sum_{t=1}^{T_{\mathrm{total}}} \sum_{n_p=1}^{N_p} \sum_{j \in \kappa} E_{\mathrm{reg\_u}}\left(t, n_p, j, \mathrm{RT}, \mathrm{HD}\right), \end{aligned} \tag{13}$$

where k_t and k_b represent traction and braking force utilization coefficients; N_p is the number of PSIs; n_p represents a PSI on the metro line and $n_p \in [1, N_p]$; $E_{\mathrm{trac}}^{n,j}(k_t, k_b, \mathrm{RT}_n)$ is total traction energy consumption in interstation n for train j; E_{aux} is energy consumed by auxiliary devices; $E_{\mathrm{reg\_u}}(t, n_p, \mathrm{RT}, \mathrm{HD})$ is the amount of utilized RBE in n_p at time step t; T_{total} is the length of operation period; κ denotes the set of trains located in the same power supply interval n_p.

Partial traction and partial braking are applied to extend the motoring and braking phases, which result in a modification on the EETC model. It is known that the efficiency of traction systems usually increases with the extent of motoring [37] and a constant efficiency factor could lead to inaccurate results [38]. Therefore, energy conversion factor η_1 in (1) is defined as a variable calculated as follows [39]:

$$\eta_1 = \begin{cases} 1 & 0.95 \le k_t < 1 \\ 0.6620 + 0.3558 \cdot k_t & 0.5 \le k_t < 0.95 \\ 0.5714 + 0.537 \cdot k_t & k_t < 0.5. \end{cases} \tag{14}$$

Due to the force utilization coefficients, (2) in Section 2.1 is rewritten as

$$\mathbf{F}\left(k_t, k_b, v, x\right) = \begin{cases} k_t \cdot F_{\mathrm{tr}}\left(v, x\right) & 0 \le x \le x_{\mathrm{cr}} \\ F_{\mathrm{cr}}\left(v, x\right) & x_{\mathrm{cr}} < x \le x_{\mathrm{co}} \\ \varphi \cdot F_{\mathrm{cr}}\left(v, x\right) & x_{\mathrm{co}} < x \le x_{\mathrm{br}} \\ -k_b \cdot F_{\mathrm{br}}\left(v, x\right) & x_{\mathrm{br}} < x \le X. \end{cases} \tag{15}$$

Then, traction energy consumption could be calculated by attaining the optimal (x_{cr}, x_{co}) in energy-efficient train control model.

The traction energy comprises not only propulsion of the train, but also consumption of auxiliary systems aboard the train such as lighting, air conditioning, and the signal system. Usually, the power of onboard auxiliary devices P_{aux} remains constant during train movements. Hence, the total energy consumption for onboard auxiliary devices is only related to the cycle time, that is, the period required for one train to complete one cycle, which is expressed as C.

$$E_{aux} = \sum_{j=1}^{J} \frac{P_{aux}^{j} C}{3600}. \tag{16}$$

The calculation of utilized RBE in each PSI during the operation period is more complex and the framework on utilization of RBE is given in Figure 6. The RBE is sequentially used to support auxiliary devices on the braking trains and traction trains in the same PSI and auxiliary devices on the other trains except braking trains. It should be noted that the regenerative energy from braking trains can only be transmitted among trains which are operating in the same PSI.

The utilization of RBE consists of two parts. The first part is used to support onboard auxiliary devices in braking trains, and the second part is used by traction trains and onboard auxiliary devices on other trains except braking trains, which is distinguished by different lines in Figure 6. Therefore, utilized RBE for all trains j in the same PSI at time step t can be calculated as

$$E_{reg\_u}(\xi) = E_{reg\_u}^{self}(\xi) + \eta_2 \cdot E_{reg\_u}^{other}(\xi), \tag{17}$$

where $\xi = \{t, n_P, j, \mathrm{RT}, \mathrm{HD} \mid 1 \le t \le T_{total}, 1 \le n_P \le N_P, j \in \kappa\}$; η_2 is the transmission loss factor of the regenerative energy.

The first part of utilized RBE which is used by braking trains is calculated by (18). If train j is braking in power supply interval n_p at time t, the vector force $\mathbf{F}$ will be negative. This means the train is providing regenerative energy. A portion of RBE is used for onboard auxiliary devices on the braking train j firstly.

$$E_{reg\_u}^{self}(\xi) = \sum_{j\in\kappa} \min\left(\eta_3 \frac{\left|\min\left(\mathbf{F}_j(v,x)\, v\Delta t, 0\right)\right|}{3600}, \frac{P_{aux}^{j}\Delta t}{3600}\right), \tag{18}$$

where η_3 denotes the conversion factor from mechanical energy to regenerative energy.

The rest of the RBE, which can be attained by (19), is available to accelerate the motoring train followed by providing power for the auxiliary devices of other trains except braking trains in the same PSI. The energy required by motoring trains is calculated by (20).

$$E_{reg}^{avai}(\xi) = \sum_{j\in\kappa} \max\left(\eta_3 \frac{\left|\min\left(\mathbf{F}_j(v,x), 0\right)\right| v\Delta t}{3600} - \frac{P_{aux}^{j}\Delta t}{3600}, 0\right) \tag{19}$$

$$Ee_{trac}(\xi) = \sum_{j\in\kappa} \frac{\max\left(\mathbf{F}_j(v,x), 0\right) v\Delta t}{3600 \cdot \eta_1}. \tag{20}$$

If the available RBE is more than the total traction energy required by motoring train in the same PSI, the surplus RBE is then used to support auxiliary devices for other trains except the braking trains in the same PSI. The total energy required by all the trains in the same PSI except the braking trains can be calculated by (21). Finally, the total utilized regenerated energy by traction trains and other trains except the braking trains is calculated in (22).

$$Ee_{aux}(\xi) = \sum_{j\in\kappa} \frac{P_{aux}^{j}\Delta t}{3600}, \quad \forall \mathbf{F}_j(v,x) \ge 0 \tag{21}$$

$$E_{reg\_u}^{others}(\xi) = \begin{cases} Ee_{trac}(\xi) + \min\left(E_{reg}^{avai}(\xi) - Ee_{trac}(\xi), Ee_{aux}(\xi)\right) & Ee_{trac}(\xi) \le E_{reg}^{avai}(\xi) \\ E_{reg}^{avai}(\xi) & Ee_{trac}(\xi) > E_{reg}^{avai}(\xi), \end{cases} \tag{22}$$

where $Ee_{aux}(\xi)$ is the total energy consumption of onboard devices of trains in the same PSI, except the braking trains.

3.2. Constraints. In this paper, we consider the operation period from the time when the first train is put into operation in the up direction to the time when the last train returns to the depot from the down direction. During the operation period, all trains have the same cycle time, traction and braking force utilization coefficients, interstation runtime, and dwell time. The constraints for energy-efficient timetable are as follows:

(1) Runtime constraints: the interstation runtime should be limited within a certain range for the consideration of service quality and the maximum traction force.

$$\underline{T_{cn}} \le T_n \le \overline{T_{cn}}, \quad \forall n \in [1, N-1] \cup [N+1, 2N-1]. \tag{23}$$

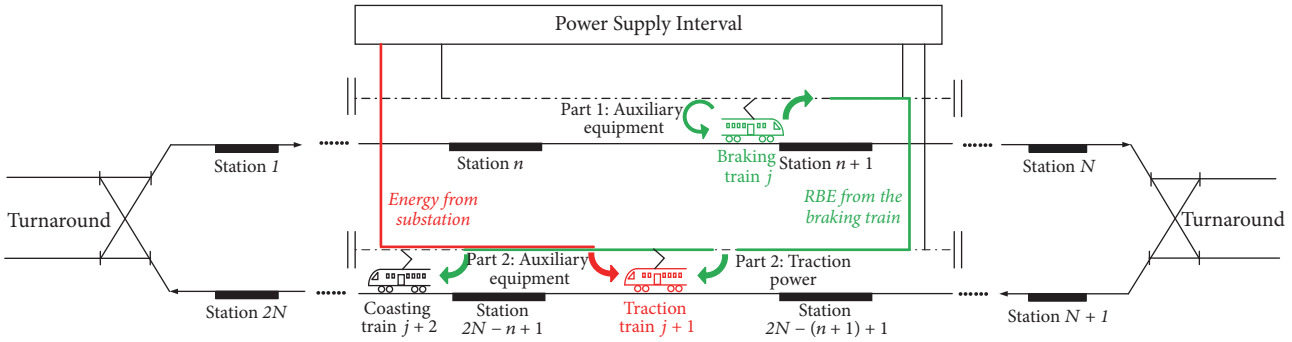

Figure 6: The utilization of regenerative braking energy.

(2) Turnaround time constraints: the turnaround time should be larger than the minimum time due to the track length of turnaround and limited travel speed, and less than a certain upper bound for the consideration of service quality and rolling stock operation.

$$\underline{T_{\text{turn}}} \le T_n \le \overline{T_{\text{turn}}}, \quad n \in \{N, 2N\}. \tag{24}$$

(3) Cycle time constraints: the total travel time for one cycle in the optimal timetable should be equal to the one in the original timetable, to keep the service frequency unchanged. In this study, we assume turnaround time as a special interstation runtime.

$$C = \sum_{n=1}^{2N} T_n + \sum_{n=1}^{2N} T_n^{\text{dwell}}. \tag{25}$$

(4) Headway constraints: the headway between any two successive trains must be less than the maximal headway required by service quality and larger than the minimal one for safety concerns.

$$\underline{H} \le H_j \le \overline{H}. \tag{26}$$

(5) Power peak: the total traction power of all trains located in the same PSI at each time moment should be no more than the maximal load of the power supply systems $P_{\text{sub}}^{\max}$.

$$\sum_j P_j(t) \le P_{\text{sub}}^{\max}. \tag{27}$$

(6) The percentages of full traction and braking force applied in motoring and braking should be limited in a reasonable range, considering the service quality requirement.

$$\begin{aligned} k_b &\in [0.5, 1] \\ k_f &\in [0.5, 1]. \end{aligned} \tag{28}$$

4. Solution Algorithm

Evolutionary algorithms, particularly the genetic algorithm (GA), have been widely adopted to solve such kind of problems especially the scheduling optimization [40–42]. However, it is easy to fall into a local solution rather than the global optimum if a standard GA is employed to solve such a complex integrated optimization problem. To improve the computing efficiency, the whole problem of energy-efficient train operation is decomposed into train trajectory formulation and timetable optimization, which are successively processed in this study. Figure 7 shows the whole structure of the optimization process.

In the single-train trajectory optimization, the brute force algorithm is applied to find the exact solution for train control with the given traction and braking force utilization coefficients as well as runtime in each interstation, and the results are saved in a database. Then, a genetic annealing algorithm with neighborhood search strategy is implemented in the integrated optimization to calculate the proper traction and braking force utilization coefficients, runtime, and headway. Train trajectories and traction energy consumption are directly taken from the database.

4.1. Brute Force Algorithms to Attain Train Trajectories. Brute force is an exact algorithm by searching all the possible solutions and evaluating their fitness, which has been successfully used in railway operation optimization [43, 44]. The main steps of brute force algorithm are as follows.

(1) Enumerating: the energy consumption and interstation runtime of all the possible solutions (x_{co}, x_{cr}) in the interstation run will be calculated, with the given force utilization coefficients (k_t, k_b) and running direction (d). The results will be stored in the database.

(2) Selection: the database may include a number of solutions with the same interstation runtime (RT), but the traction energy consumption is different. For each runtime, only the solution with the least traction energy consumption will be retained and other solutions with the same runtime will be removed from the database.

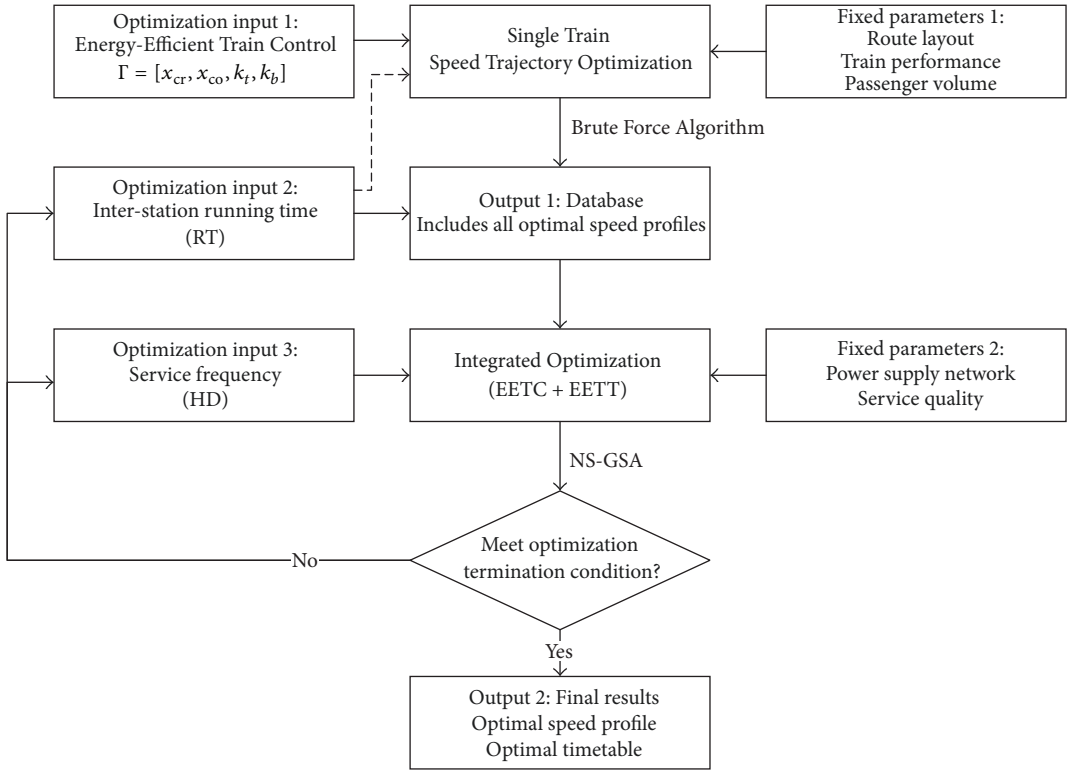

Figure 7: Flowchart of the integrated optimization.

(3) Updating: the force utilization coefficients (k_t, k_b) and running direction (d) will be updated, while the value should satisfy the constraint in (28). Then, the algorithm returns back to Step (1). If all the possible combinations of k_t, k_b, and d in this interstation are calculated, go to Step (4).

(4) Termination: the optimal train control schemes in the interstation with different runtimes, running directions, traction force utilization coefficients k_t, and braking force utilization coefficients k_b are obtained and stored in the database.

The algorithm takes about 1.1 hours to generate a database for one interstation, which gives the optimal solutions and the corresponding energy performance under 2160 different operation conditions, involving 6 traction coefficients, 6 braking coefficients, 30 runtimes, and 2 run directions.

4.2. NS-GSA Algorithm in Timetable Optimization. An improved genetic annealing algorithm with neighborhood search strategy (NS-GSA) is used to optimize the timetable. To overcome the premature convergence in the standard genetic algorithm, a simulated annealing (SA) algorithm is introduced to escape from the local optimum and approach the global optimum. Metropolis criterion of simulated annealing (SA) allows a decreasing probability of accepting worse solutions, which provides a diverse population for GA without compromising solution convergence. Additionally, the solution space is quite large in this integrated optimization problem, and the variables are continuous. Therefore, it is necessary to enhance the local search ability of genetic simulated annealing (GSA) algorithm, and neighborhood search strategy (or local search) is used which has been proved to be an effective search technique and is widely implemented in railway operation and management [45–48]. The procedure of NS-GSA is shown in Figure 8.

The main steps of the developed algorithm are as follows:

(1) Initialization: a random initial population of the solutions is produced to form the first generation. A number of individuals are included in the population and each individual represents a set of traction force utilization coefficient (k_t), braking force utilization coefficient (k_b), interstation runtime (RT), and headway (HD), which are the decision variables in the integrated optimization model.

(2) Neighborhood search: each individual explores its neighborhood to enhance the local search ability of the algorithm. The details on neighborhood search are presented below.

   (a) Initialize the set of neighborhood structures SOL(p, q), $p \in \{1, \ldots, P\}$, $q \in \{1, \ldots, Q\}$. P is the number of individuals and Q is the maximum number of local searches for each individual. Set $p = 1$, $q = 1$.

   (b) Until $q = Q + 1$, repeat the following operations. Through randomly generating a set of RT within a reasonable range, a set of solutions SOL(p, q) in the neighborhood of SOL(p) is

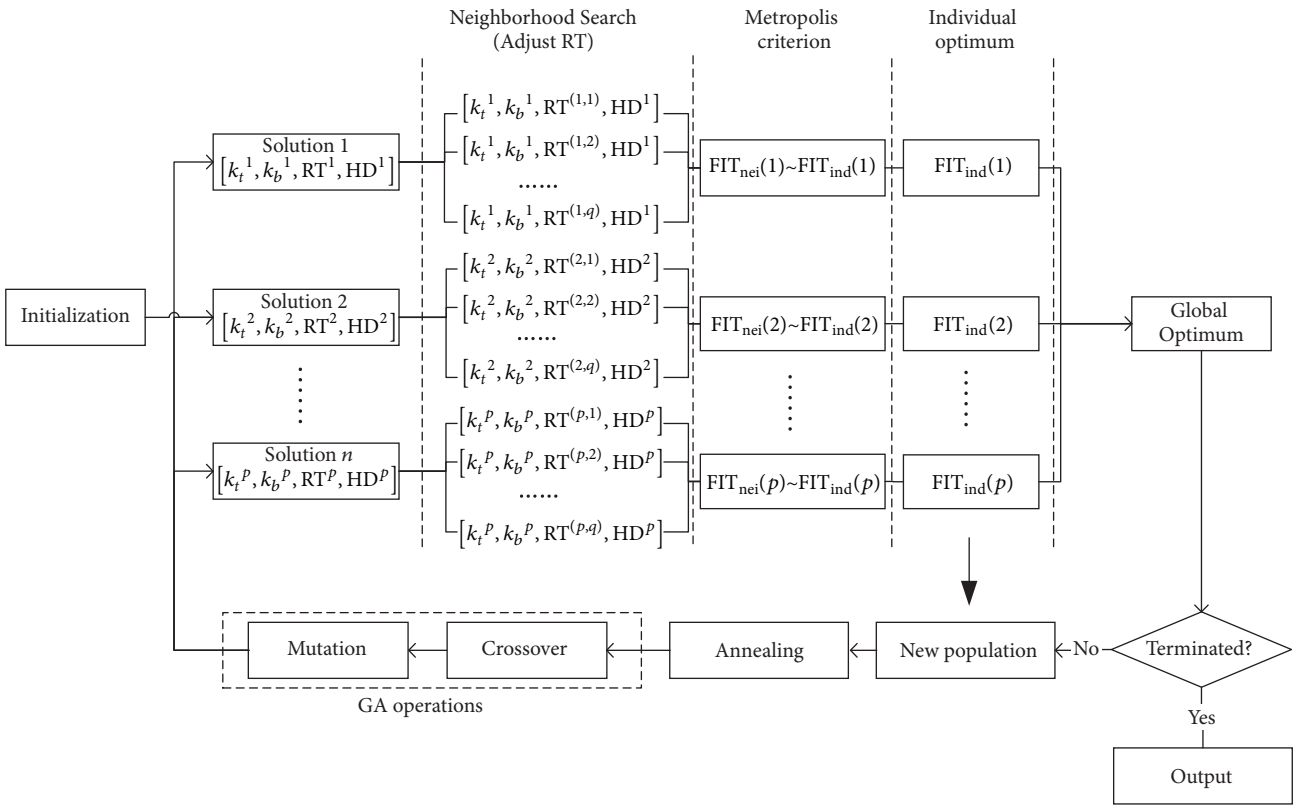

Figure 8: Flowchart of NS-GSA algorithm.

produced by replacing the RT in SOL(p) with the newly generated RT. It should be noted that the journey time should not be changed in each local searching. Set $q \leftarrow q + 1$.

(c) Set $p \leftarrow p+1$. If $p > P$, finish the neighborhood search. Otherwise, set $q = 1$ and go to Step (b).

(3) Evaluation: each solution in the population will be evaluated. Equation (13) is used to calculate the fitness FIT(p, q) of solution SOL(p, q).

(4) Acceptance: if the best neighborhood solution of the individual p with the fitness $FIT_{nei}(p)$ is better than the individual fitness $FIT_{ind}(p)$, the individual will be replaced by the neighborhood solution. Otherwise, the individual will be replaced by the best neighborhood solution according to the Metropolis criterion in simulated annealing algorithm. The acceptance criterion is listed as follows:

$$\begin{aligned} &\forall p \in P, \text{if } FIT_{nei}(p) < FIT_{ind}(p) \\ &FIT_{ind}(p) = FIT_{nei}(p) \\ &\text{elseif } e^{(FIT_{ind}(p) - FIT_{nei}(p))/Temper} < Rand(0,1) \\ &FIT_{ind}(p) = FIT_{nei}(p). \end{aligned} \tag{29}$$

(5) New generation: if the termination conditions are not satisfied, the optimal individuals after neighborhood searching will be used to create a new generation. The parameter Temper in Metropolis criterion decreases at a certain rate at the same time.

(6) Crossover: set the random number k_c ($0 \le k_c \le 1$) and the probability of crossover P_c. If $k_c \le P_c$, then crossover operation will randomly select three positions of genes in three parts of the chromosome, corresponding to force utilization coefficients, interstation runtime, and headway. Then, two chromosomes in the population will exchange these genes. As shown in Figure 9, genes which have been exchanged in crossover are marked in green.

(7) Mutation: set random number k_m ($0 \le k_m \le 1$) and the probability of crossover P_m. If $k_m \le P_m$, the mutation operation will randomly select one gene from one chromosome and replace the gene with a random number within the reasonable range. It should be noted that constraints in Sections 2.2 and 3.2 should be satisfied.

(8) Termination: the algorithm returns to Step (2) and repeats until the maximum generation is reached.

The required CPU time of NS-GSA algorithm is about 20 hours to attain the energy-efficient timetable as well as the optimal control schemes using a computer with 3.2 GHz processor speed and 4 GB memory, when the number of individuals in GA is 20, the number of neighborhood solutions for each individual is 2, and the maximum generation is 40.

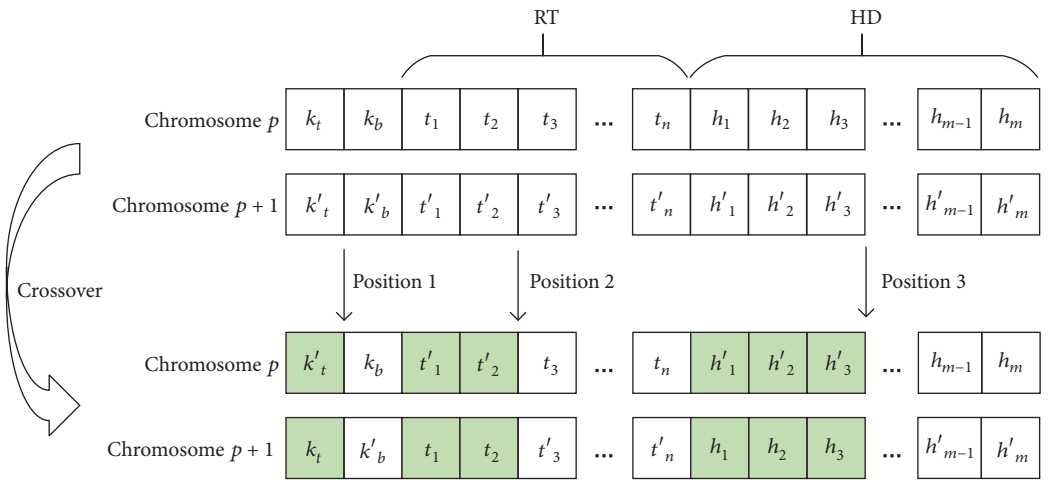

FIGURE 9: The structure of chromosome and crossover operation.

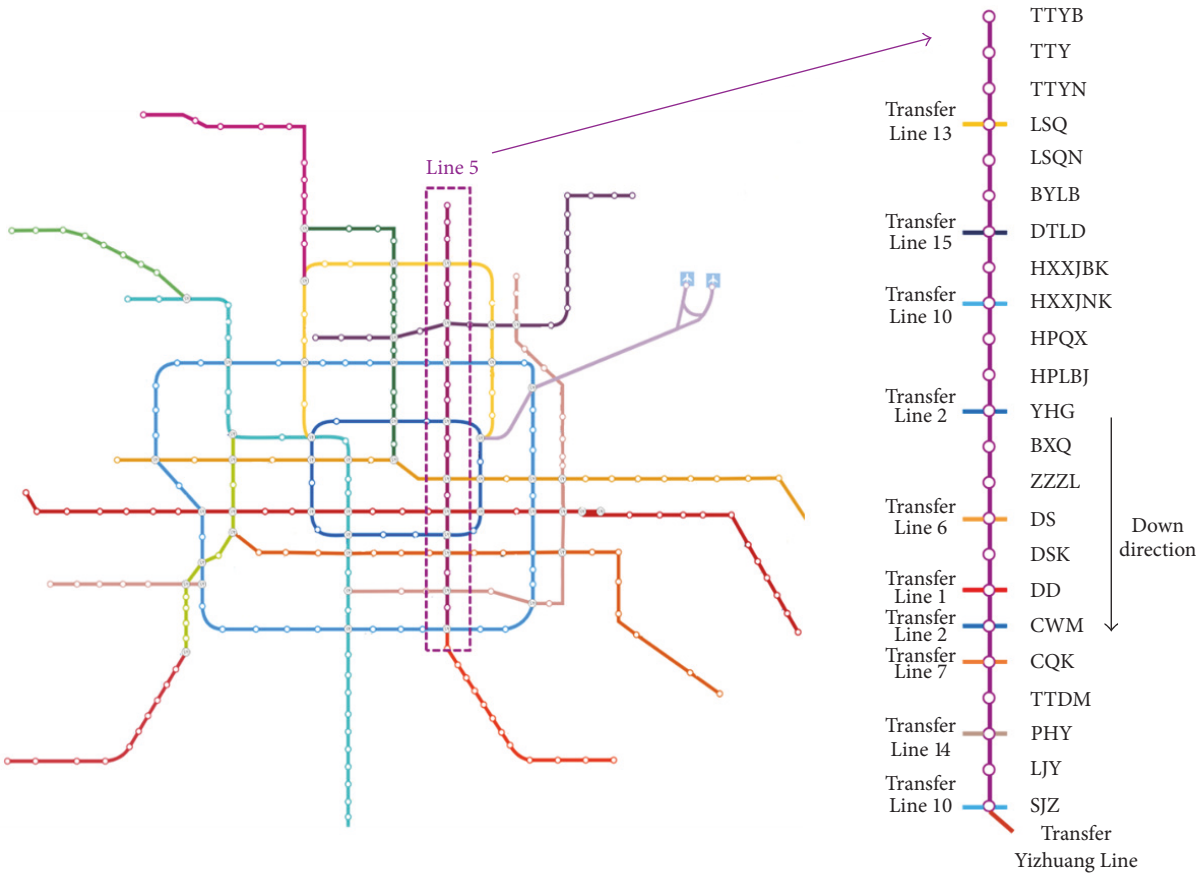

FIGURE 10: Beijing Metro network and Line 5.

5. Case Study

In this section, case studies on Beijing Metro Line 5 in peak hours are employed to illustrate the effectiveness of the improved train control and integrated optimization model.

5.1. Basic Data. The Beijing Metro Line 5 is 27.6 km long with 23 stations. It covers several commercial centers and links the residential districts in north and south of Beijing (see Figure 10). Table 2 gives the basic information of trains servicing on Beijing Metro Line 5 and Figure 11 shows the traction and regenerative braking characteristics of the train.

The number of passengers on the train in different interstation runs is shown in Figure 12, taking peak hour as an example. It is used to attain train mass, assuming the mass of each person is 60 kg. There are 11 PSIs on Beijing Metro

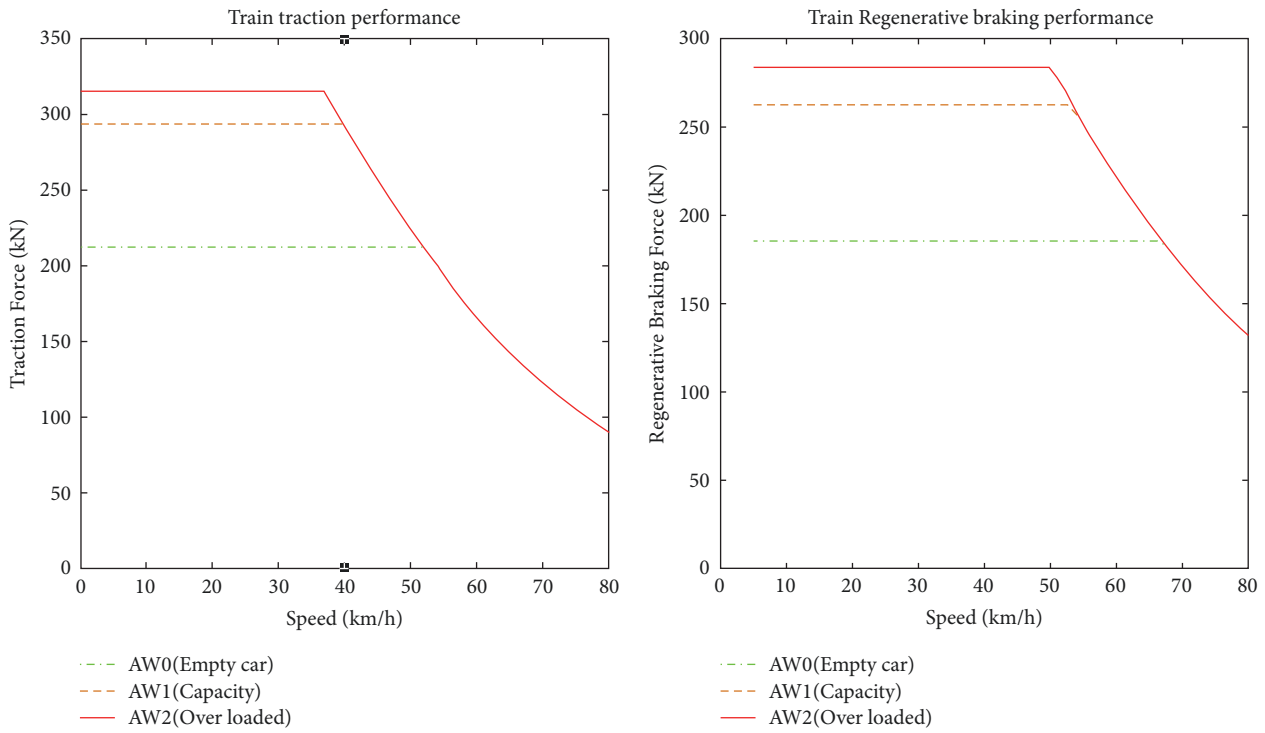

Figure 11: The power performance under different load factors.

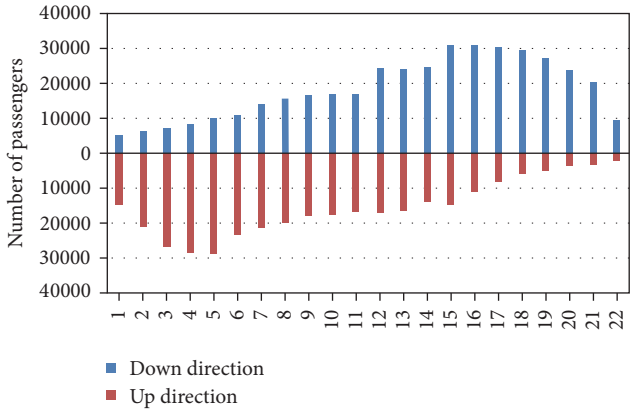

Figure 12: Number of passengers on the train in different interstations.

Table 2: Train characteristics.

Rolling stock mass	203,000 kg
Max speed limit	80 km/h
Number of cars	6 pcs
Maximum acceleration	1.0 m/s^2
Maximum deceleration	–1.0 m/s^2
Minimum speed for RBE	5 km/h
Resistance coefficient a	1.2414
Resistance coefficient b	0.0144
Resistance coefficient c	0.000221

Line 5, and power peak in every PSI is 8500 kW. For safety and quality of service, the maximal headway is 160 s and the minimal headway is 140 s. In the NS-GSA solution algorithm, we set population $P = 100$, $Q = 10$, $P_c = 0.8$, $P_m = 0.1$, the maximum generation as 50, and the annealing rate as 0.95 with an initial temperature of 100°C.

5.2. Energy Performance of Improved Energy-Efficient Train Control. Table 3 gives the energy performance of the improved model (MA-[CR-CO]$_n$-MB) and previous model (MA-CR-CO-MB) with the same runtime, from DTLD to HXXJNK in down direction. The improved train control strategy is able to reduce traction energy consumption by 1.07 kWh in the first interstation with steep downhill slopes and the potential annual traction energy saving in this interstation could be up to 50772 kWh. On the other hand, two driving strategies consumed the same traction energy in the second interstation where there is no steep downhill slope.

Figure 13 demonstrates the train trajectories of two driving strategies to further explain the reason of traction energy reduction by improved control model in a more intuitive way. In the first interstation, the trajectory obtained by the improved control consists of MA-[CR-CO]$_2$-MB; both CR and CO are implemented twice but the second CO is omitted because MB has to be implemented for station stop. In contrast, the trajectory attained by the previous model is sequentially composed of MA, CR, CO, and MB. The improved trajectory extends the coasting distance in steep downhill tracks in order to take full advantage of potential energy to increase the kinetic energy. As such, MA can be

Table 3: Energy performance of the improved train control model.

Interstation	DTLD-HXXJBK (with steep downhills)		HXXJBK-HXXJNK (without a steep downhill)	
Driving strategy	Improved	MA-CR-CO-MB	Improved	MA-CR-CO-MB
Runtime (s)	129	129	94	94
Traction energy consumption (kWh)	6.42	7.49	6.09	6.09

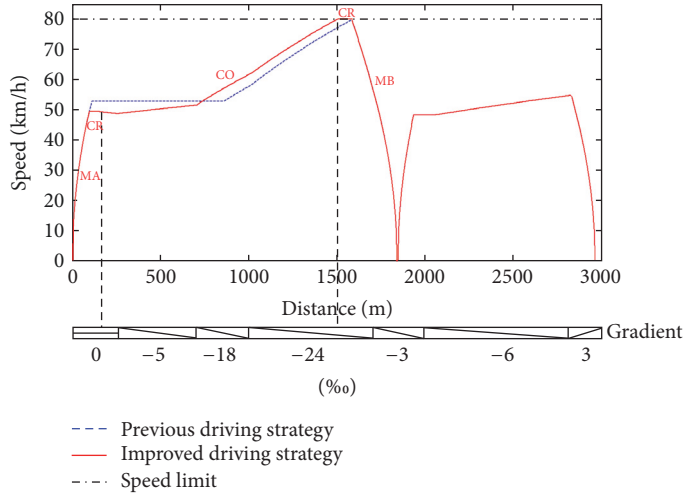

Figure 13: The comparison between two driving strategies.

shortened and the traction energy consumption is saved, while the interstation runtime remains the same. In the second interstation, two control strategies obtained the same trajectory as well as the traction energy consumption, as there is no steep downhill track in this interstation.

It can be concluded that the traction energy performance of the improved control strategy is better than or equal to the MA-CR-CO-MB strategy. Additionally, runtime supplements in each interstation run have significant influences on train trajectory optimization. We studied the energy-saving rates of the improved train control in comparison with the previous model under different runtimes. Figure 14 shows traction energy consumption of two control strategies in interstation DTLD-HXXJNK with different runtimes.

When the scheduled runtime is equal to the minimum interstation runtime, the train has to accelerate to speed limit using maximum traction force and keep the speed constant to satisfy the runtime constraint until the train brakes for station stop. Under this condition, two control strategies attained the same trajectory and consumed the same energy because there is no room to apply CO. Along with the increment of runtime supplements, the improved train control can realize increased energy saving because more CR is allowed in downhill sections, which reduces the traction energy consumption by taking advantage of potential energy. Once the interstation runtime reaches a certain level, the energy-saving ratio decreases because the motoring distances in both control strategies decrease. In case the scheduled runtime is large enough, the trajectories as well as the energy consumption of the two models are the same.

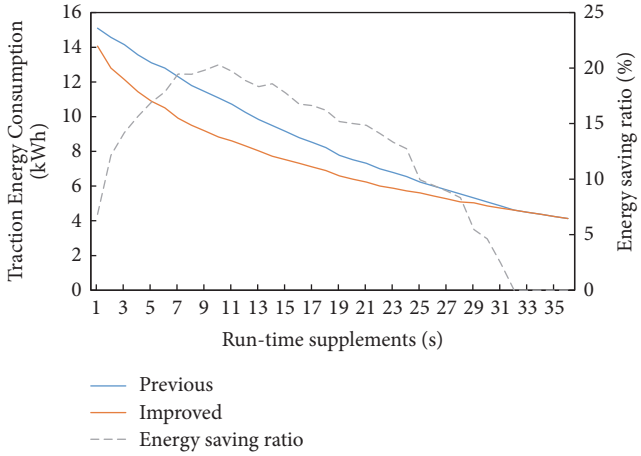

Figure 14: Energy-saving effect of the improved driving strategy at different runtimes.

In addition to interstation runtime and track profile, train mass also has a great impact on traction energy consumption because a large mass results in heavier resistance during the interstation runs and also helps the train accelerate in downhill slopes. We used the proposed control strategy and the one applied in previous studies to obtain the optimal trajectories in the interstation DTLD-HXXJBK, with different train masses and different interstation runtimes. The traction energy reduction by the improved control in comparison with the previous model is shown in Figure 15. It is found that

Table 4: The original timetable and the optimized timetable.

ID	Interstation	Length (m)	Up direction			Down direction			PSI
			Runtime (s)		Dwell time (s)	Runtime (s)		Dwell time (s)	
			Original	Optimized		Original	Optimized		
1	SJZ-LJY	1671	126	122	45	130	123		1
2	LJY-PHY	905	81	92	30	82	88	41	
3	PHY-TTDM	1900	133	140	30	133	127	30	2
4	TTDM-CQK	1183	98	96	45	97	92	30	3
5	CQK-CWM	877	80	80	50	79	84	45	
6	CWM-DD	822	79	92	60	79	75	50	
7	DD-DSK	945	83	93	30	82	88	60	4
8	DSK-DS	848	81	82	45	81	88	30	
9	DS-ZZZL	1017	89	86	30	87	84	45	5
10	ZZZL-BXQ	791	78	82	30	74	75	30	
11	BXQ-YHG	866	81	88	50	85	86	30	
12	YHG-HPLBJ	1151	98	96	30	103	91	50	6
13	HPLBJ-HPXQ	1059	93	90	30	93	91	30	
14	HPXQ-HXXJNK	1025	89	87	55	91	87	30	7
15	HXXKNK-HXXJBK	1122	99	92	30	94	97	55	
16	HXXJBK-DTLD	1838	133	137	40	129	127	30	8
17	DTLD-BYLB	3000	180	180	30	181	181	40	9
18	BYLB-LSQN	1286	110	110	30	108	100	30	10
19	LSQN-LSQ	1306	111	109	50	112	112	30	
20	LSQ-TTYN	1544	120	109	30	119	111	50	11
21	TTYN-TTY	966	86	93	30	86	84	30	
22	TTY-TTYB	939	85	94		86	85	40	
Total		27061	2213	2250	800	2211	2176	806	

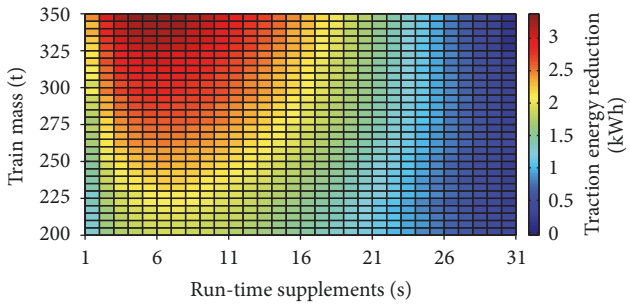

Figure 15: Traction energy reduction under various conditions using improved driving strategies.

the improved model achieves better energy saving when the train mass increases. The reason is that heavier trains acquire greater acceleration when coasting in steep downhills, and they can gain higher kinetic energy in steep downhill tracks and achieve better energy saving.

To sum up, the improved model is a supplement to the MA-CR-CO-MB control strategy in interstations with constant speed limit and it is able to save traction energy in downhill sections by taking advantage of potential energy. Energy saving is influenced by the scheduled runtime and train mass. The energy saving firstly increases with scheduled runtime and then decreases, finally reaching zero when the runtime is sufficient. Heavier trains can achieve a better traction energy reduction because the acceleration is larger when the train is coasting in downhills where the potential energy could help the train more in accelerating.

5.3. Energy Performance of Integrated Optimization. Separate train control to minimize the traction energy consumption of each train does not necessarily lead to the minimum net energy consumption of whole metro lines. The energy consumption of the whole metro lines can be further reduced by optimizing train control and timetable concurrently. Table 4 shows the original timetable and train control configurations (RT, HD, k_t, and k_b) provided by operators and the optimized one obtained by the proposed integrated optimization model. The original journey time is 2213 s in the up direction and 2211 s in the down direction. Compared with the original timetable, the optimized timetable increases by 37 s in the up direction and decreases by 35 s in the down direction. Therefore, the cycle time is extended by 2 s, which is acceptable. Additionally, train headway is regulated to improve the utilization of RBE. The headway is set as a fixed value (i.e., 150 s) in the original timetable. In the optimized one, the headway between every two adjacent trains varies within a reasonable range from 140 s to 159 s, without changing the number of service provisions and dwell time at each station.

Table 5: Comparison of energy consumption between the original timetable and optimized timetable.

	Original timetable	Optimized timetable	
$[k_t, k_b]$	[1, 1]	[0.9, 0.9]	
Net energy consumption (kWh)	15059	14311	(−4.97%)
Auxiliary devices (kWh)	530	530	(+0.00%)
Traction energy (kWh)	16567	17554	(+5.96%)
Total RBE (kWh)	13016	14360	(+10.33%)
Utilized RBE (kWh)			
Auxiliary (self)	52	57	(+9.62%)
Traction	1840	3570	(+94.02%)
Auxiliary (other)	146	147	(+0.68%)
Total	2038	3773	(+85.13%)
Overlapping time (s)	4194	4543	(+8.32%)
Utilization percentage of RBE (%)	15.66	26.27	(+67.81%)

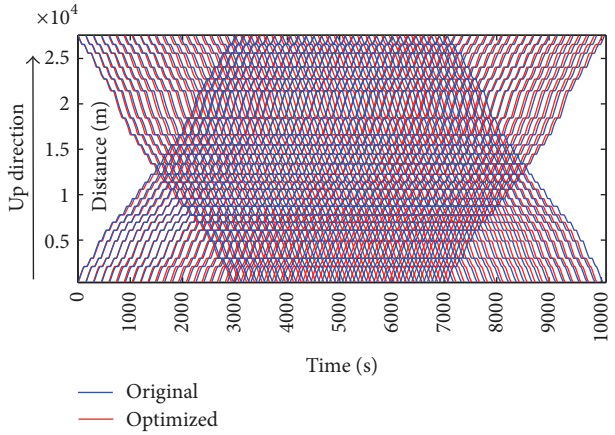

Figure 16: Comparison of the original and optimal timetable.

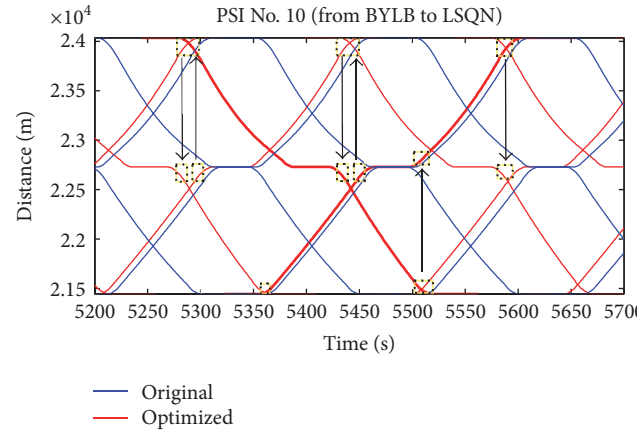

Figure 17: The utilization of the regenerative braking energy in the same power supply interval.

Table 5 shows the comparison of energy consumption between the original timetable with previous train control model and the optimized timetable with the improved train control model. Although traction energy consumption with the optimized timetable increases by 5.96%, the net energy consumption of the whole line decreases by 4.97% because of the significant improvements on utilization of RBE. This verifies the argument that minimum traction energy consumption does not necessarily lead to the minimum net energy consumption. Although partial traction and braking result in a slight increment in traction energy consumption, the utilization of RBE with the optimized timetable increases by 67.81% as the overlapping time increases by 8.32%. It is concluded that the integrated optimization model can notably improve the utilization of RBE, thus reducing the net energy consumption.

Figure 16 shows the difference between the original timetable and the optimized timetable. The total journey time and the operating time for service provision remain the same in the optimized timetable, although the interstation runtime (RT) and train headway (HD) are regulated slightly.

An enlarged view of part of Figure 16, taking a section from the station of BYLB to the station of LSQ in the same PSI as an example, is shown in Figure 17 to explicate how the utilization of RBE is optimized by the integrated model. The arrows in the figure illustrate the flow of regenerative braking energy; that is, the RBE generated by the braking train can be transmitted to the traction train. It is found that motoring and braking of trains in the same PSI could be synchronized by adjusting headway and interstation runtime in timetable formulation. Moreover, overlapping time could be further extended using partial traction/braking to prolong the motoring and braking time. As a result, the net energy consumption decreases, although the traction energy consumption is not the minimal one.

Figure 18 gives the trajectories of two successive trains moving in the same PSI. Under the original timetable with full motoring and braking control, the RBE is not used timely because motoring train and braking train are not synchronized well. By optimizing headway and interstation runtime, the departure of train 2 from DD station just located in the same time window when train 1 arrives at the TTDM station. Furthermore, the synchronized time between traction and braking train is prolonged by applying partial motoring and braking, which enable a larger overlapping

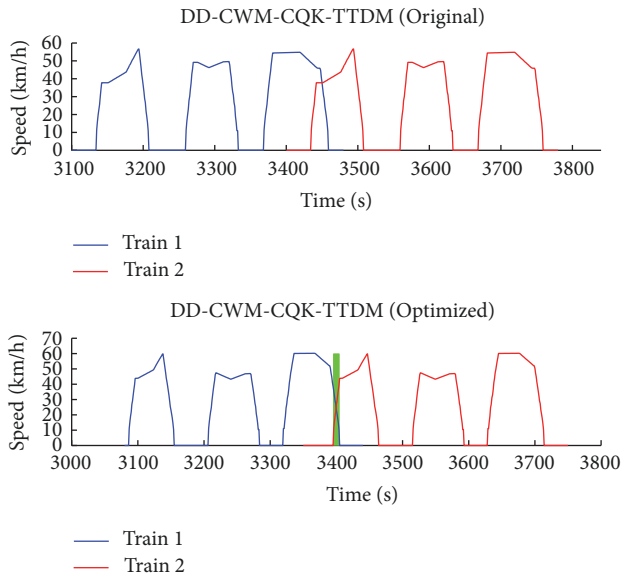

Figure 18: Synchronized traction and braking train in one power supply interval.

time as well as a better utilization of RBE. Thus, most of the RBE produced by train 1 is timely used by train 2, which helps to reduce the energy feeding from substations and in turn save the net energy consumption of the whole metro line.

6. Conclusion

An integrated optimization model on train control and timetable formulation is proposed in this study to minimize the net energy consumption of all trains servicing on the metro line. The proposed train control is still based on finding the optimal switching points among the control modes of MA, CR, CO, and MB to minimize the traction energy consumption, while cruising and coasting regimes might be adopted for more than one time according to track profiles. For better utilization of RBE, timetable configurations such as interstation runtime and train headway as well as the extents of motoring and braking in train control are optimized concurrently, taking into account the synchronization of motoring and braking trains in the same PSI. Practical operation condition and constraints, such as varied train mass in different interstations, the limitation on maximal loading of power system, are taken into consideration in the proposed model. The brute force algorithm is employed to attain the energy-efficient trajectory of train interstation runs and an NS-GSA algorithm is developed to attain the optimal extents of motoring/braking and timetable configurations.

Case studies on Beijing Metro Line 5 demonstrated the energy performance of the proposed integrated model. It is found that the improved train control can reduce the traction energy by 20% in the interstations with steep downhill slopes. The energy-saving rate of the improved train control in comparison with the previous model depends on track profiles and the scheduled runtime. The integrated optimization on train control and timetable formulation is able to save net energy consumption by 4.97% through regulating interstation runtime, train headway, and the extents of motoring and braking in train control. Although the traction energy slightly increases by 5.96% because of the application of partial motoring and braking in train control, the utilization of RBE is significantly improved by prolonging the overlapping time of motoring and braking trains in the same PSI.

This paper explored the energy-efficient train control with the constant speed limit, while the speed limit may vary during interstation runs due to curves or temporary maintenance. In such case, the proposed control strategy might not be the optimal one. One of our future researches is to take the varied speed limits into consideration in train control and apply a more general energy-efficient train control model in timetable optimization. Additionally, this study assumes that all trains have the same extents of motoring and braking in different interstation runs. Different extents of motoring and braking for different trains in different interstation runs might lead to more significant energy savings, which is another direction of future research.

Conflicts of Interest

The authors declare that they have no conflicts of interest.

Acknowledgments

This work was supported by the National Natural Science Foundation of China (71390332, 71621001, and 71571016) and the Fundamental Research Funds for the Central Universities (2016JBM031).

References

[1] A. González-Gil, R. Palacin, P. Batty, and J. P. Powell, "A systems approach to reduce urban rail energy consumption," *Energy Conversion and Management*, vol. 80, pp. 509–524, 2014.

[2] K. Ichikawa, "Application of optimization theory for bounded state variable problems to the operation of train," *Journal of the Japan Society of Mechanical Engineers*, vol. 11, no. 47, pp. 857–865, 1968.

[3] H. Strobel, P. Horn, and M. Kosemund, "A contribution to optimum computer-aided control of train operation," in *Proceedings of the 2nd FAC/IFIP/IFORS Symposium on Traffic Control and Transportation Systems*, pp. 377–387, 1974.

[4] I. P. Milroy, *Aspect of automatics train control [Ph.D. dissertation]*, Loughborough University of Technology, Sydney, Australia, 1980.

[5] B. R. Benjamin, A. M. Long, I. P. Milroy, R. L. Payne, and P. J. Pudney, "Control of railway vehicles for energy conservation and improved timekeeping," in *Proceedings of the Conference on Railway Engineering*, pp. 41–47, Perth, Australia, 1987.

[6] P. G. Howlett, I. P. Milroy, and P. J. Pudney, "Energy-efficient train control," *Control Engineering Practice*, vol. 2, no. 2, pp. 193–200, 1994.

[7] E. Khmelnitsky, "On an optimal control problem of train operation," *IEEE Transactions on Automatic Control*, vol. 45, no. 7, pp. 1257–1266, 2000.

[8] R. Liu and I. M. Golovitcher, "Energy-efficient operation of rail vehicles," *Transportation Research Part A: Policy and Practice*, vol. 37, no. 10, pp. 917–932, 2003.

[9] L. A. M. V. Dongen and J. H. Schuit, "Energy-efficient driving patterns in electric railway traction," in *Proceedings of the International Conference on Main Line Railway Electrification (IET '02)*, pp. 154–158, 2002.

[10] G. M. Scheepmaker and R. M. P. Goverde, "The interplay between energy-efficient train control and scheduled running time supplements," *Journal of Rail Transport Planning and Management*, vol. 5, no. 4, pp. 225–239, 2015.

[11] P. G. Howlett, P. J. Pudney, and X. Vu, "Local energy minimization in optimal train control," *Automatica*, vol. 45, no. 11, pp. 2692–2698, 2009.

[12] Y. Bai, B. H. Mao, F. M. Zhou, Y. Ding, and C. B. Dong, "Energy-efficient driving strategy for freight trains based on power consumption analysis," *Journal of Transportation Systems Engineering & Information Technology*, vol. 9, no. 3, pp. 43–50, 2009.

[13] M. Domínguez, A. Fernández-Cardador, A. P. Cucala, T. Gonsalves, and A. Fernández, "Multi objective particle swarm optimization algorithm for the design of efficient ATO speed profiles in metro lines," *Engineering Applications of Artificial Intelligence*, vol. 29, pp. 43–53, 2014.

[14] W. Carvajal-Carreño, A. P. Cucala, and A. Fernández-Cardador, "Optimal design of energy-efficient ATO CBTC driving for metro lines based on NSGA-II with fuzzy parameters," *Engineering Applications of Artificial Intelligence*, vol. 36, pp. 164–177, 2014.

[15] C. Sicre, A. P. Cucala, and A. Fernández-Cardador, "Real time regulation of efficient driving of high speed trains based on a genetic algorithm and a fuzzy model of manual driving," *Engineering Applications of Artificial Intelligence*, vol. 29, no. 29, pp. 79–92, 2014.

[16] K. Keskin and A. Karamancioglu, "Energy-efficient train operation using nature-inspired algorithms," *Journal of Advanced Transportation*, vol. 2017, Article ID 6173795, 12 pages, 2017.

[17] W. Shangguan, X.-H. Yan, B.-G. Cai, and J. Wang, "Multiobjective optimization for train speed trajectory in CTCS high-speed railway with hybrid evolutionary algorithm," *IEEE Transactions on Intelligent Transportation Systems*, vol. 16, no. 4, pp. 2215–2225, 2015.

[18] T. Albrecht and S. Oettich, *A New Integrated Approach to Dynamic Schedule Synchronization and Energy-Saving Train Control*, WIT Press, Southampton, UK, 2002.

[19] C. Sicre, P. Cucala, A. Fernández, J. A. Jiménez, I. Ribera, and A. Serrano, "A method to optimise train energy consumption combining manual energy efficient driving and scheduling," in *Proceedings of the 12th International Conference on Computer System Design and Operation in the Railways and other Transit Systems (COMPRAIL '10)*, pp. 549–560, September 2010.

[20] R. Chevrier, P. Pellegrini, and J. Rodriguez, "Energy saving in railway timetabling: a bi-objective evolutionary approach for computing alternative running times," *Transportation Research Part C: Emerging Technologies*, vol. 37, pp. 20–41, 2013.

[21] G. M. Scheepmaker, R. M. Goverde, and L. Kroon, "Review of energy-efficient train control and timetabling," *European Journal of Operational Research*, vol. 257, no. 2, pp. 355–376, 2017.

[22] R. Barrero, J. van Mierlo, and X. Tackoen, "Energy savings in public transport," *IEEE Vehicular Technology Magazine*, vol. 3, no. 3, pp. 26–36, 2008.

[23] T. Albrecht, "Reducing power peaks and energy consumption in rail transit systems by simultaneous train running time control," *Computers in Railways*, pp. 885–894, 2004.

[24] X. Yang, X. Li, Z. Gao, H. Wang, and T. Tang, "A cooperative scheduling model for timetable optimization in subway systems," *IEEE Transactions on Intelligent Transportation Systems*, vol. 14, no. 1, pp. 438–447, 2013.

[25] X. Yang, B. Ning, X. Li, and T. Tang, "A two-objective timetable optimization model in subway systems," *IEEE Transactions on Intelligent Transportation Systems*, vol. 15, no. 5, pp. 1913–1921, 2014.

[26] Z. Le, K. Li, J. Ye J, and X. Xu, "Optimizing the train timetable for a subway system," *Proceedings of the Institution of Mechanical Engineers Part F: Journal of Rail & Rapid Transit*, vol. 229, no. 8, pp. 2532–2542, 2015.

[27] M. Peña-Alcaraz, A. Fernández, A. P. Cucala, A. Ramos, and R. R. Pecharromán, "Optimal underground timetable design based on power flow for maximizing the use of regenerative-braking energy," *Proceedings of the Institution of Mechanical Engineers, Part F: Journal of Rail and Rapid Transit*, vol. 226, no. 4, pp. 397–408, 2011.

[28] Y. Ding, H. D. Liu, Y. Bai, and F. M. Zhou, "A two-level optimization model and algorithm for energy-efficient urban train operation," *Journal of Transportation Systems Engineering & Information Technology*, vol. 11, no. 1, pp. 96–101, 2011.

[29] S. Su, X. Li, T. Tang, and Z. Gao, "A subway train timetable optimization approach based on energy-efficient operation strategy," *IEEE Transactions on Intelligent Transportation Systems*, vol. 14, no. 2, pp. 883–893, 2013.

[30] S. Su, T. Tang, X. Li, and Z. Gao, "Optimization of multitrain operations in a subway system," *IEEE Transactions on Intelligent Transportation Systems*, vol. 15, no. 2, pp. 673–684, 2014.

[31] X. Yang, A. Chen, B. Ning, and T. Tang, "A stochastic model for the integrated optimization on metro timetable and speed profile with uncertain train mass," *Transportation Research Part B: Methodological*, vol. 91, pp. 424–445, 2016.

[32] X. Li and H. K. Lo, "An energy-efficient scheduling and speed control approach for metro rail operations," *Transportation Research Part B: Methodological*, vol. 64, pp. 73–89, 2014.

[33] N. Zhao, C. Roberts, S. Hillmansen, Z. Tian, P. Weston, and L. Chen, "An integrated metro operation optimization to minimize energy consumption," *Transportation Research Part C: Emerging Technologies*, vol. 75, pp. 168–182, 2017.

[34] S. Su, T. Tang, and Y. H. Wang, "Evaluation of strategies to reducing traction energy consumption of metro systems using an optimal train control simulation model," *Energies*, vol. 9, no. 2, pp. 105–123, 2016.

[35] S. Watanabe and T. Koseki, "Energy-saving train scheduling diagram for automatically operated electric railway," *Journal of Rail Transport Planning and Management*, vol. 5, no. 3, pp. 183–193, 2015.

[36] M. Miyatake and H. Ko, "Optimization of train speed profile for minimum energy consumption," *IEEJ Transactions on Electrical and Electronic Engineering*, vol. 5, no. 3, pp. 263–269, 2010.

[37] A. Albrecht, P. Howlett, P. Pudney, X. Vu, P. Zhou, and D. Chen, "Using maximum power to save energy," in *Proceedings of the 17th IEEE International Conference on Intelligent Transportation Systems*, pp. 1205–1208, Qingdao, China, November 2014.

[38] Á. J. López-López, R. R. Pecharromán, A. Fernández-Cardador, and A. P. Cucala, "Assessment of energy-saving techniques in direct-current-electrified mass transit systems," *Transportation Research Part C: Emerging Technologies*, vol. 38, pp. 85–100, 2014.

[39] M. Domínguez, A. Fernández, A. P. Cucala, and P. Lukaszewicz, "Optimal design of metro automatic train operation speed

profiles for reducing energy consumption," *Proceedings of the Institution of Mechanical Engineers, Part F: Journal of Rail and Rapid Transit*, vol. 225, no. 5, pp. 463–474, 2011.

[40] A. P. Cucala, A. Fernández, C. Sicre, and M. Domínguez, "Fuzzy optimal schedule of high speed train operation to minimize energy consumption with uncertain delays and drivers behavioral response," *Engineering Applications of Artificial Intelligence*, vol. 25, no. 8, pp. 1548–1557, 2012.

[41] X. Yang, X. Li, B. Ning, and T. Tang, "An optimisation method for train scheduling with minimum energy consumption and travel time in metro rail systems," *Transportmetrica B: Transport Dynamics*, vol. 3, no. 2, pp. 79–98, 2015.

[42] P. Shrivastava, S. L. Dhingra, and P. J. Gundaliya, "Application of genetic algorithm for scheduling and schedule coordination problems," *Journal of Advanced Transportation*, vol. 36, no. 1, pp. 23–41, 2002.

[43] B. Fan, C. Roberts, and P. Weston, "A comparison of algorithms for minimising delay costs in disturbed railway traffic scenarios," *Journal of Rail Transport Planning and Management*, vol. 2, no. 1-2, pp. 23–33, 2012.

[44] N. Zhao, C. Roberts, S. Hillmansen, and G. Nicholson, "A multiple train trajectory optimization to minimize energy consumption and delay," *IEEE Transactions on Intelligent Transportation Systems*, vol. 16, no. 5, pp. 2363–2372, 2015.

[45] S. Yang, K. Yang, Z. Gao, L. Yang, and J. Shi, "Last-train timetabling under transfer demand uncertainty: mean-variance model and heuristic solution," *Journal of Advanced Transportation*, vol. 2017, Article ID 5095021, 13 pages, 2017.

[46] M. Samà, A. D'Ariano, F. Corman, and D. Pacciarelli, "A variable neighbourhood search for fast train scheduling and routing during disturbed railway traffic situations," *Computers & Operations Research*, vol. 78, pp. 480–499, 2017.

[47] A. D'Ariano, F. Corman, D. Pacciarelli, and M. Pranzo, "Reordering and local rerouting strategies to manage train traffic in real time," *Transportation Science*, vol. 42, no. 4, pp. 405–419, 2008.

[48] P. Pellegrini and M. Birattari, "Implementation effort and performance," in *Engineering Stochastic Local Search Algorithms. Designing, Implementing and Analyzing Effective Heuristics, International Workshop, SLS 2007, Brussels, Belgium, September 2007*, Springer, 2007.